Phase Noise Measurements of the 400-kW, 2.115-GHz (S-Band) Transmitter

P. Boss, D. Hoppe, and A. Bhanji
Radio Frequency and Microwave Subsystems Section

This article describes the measurement theory and presents a test method to perform phase noise verification using off-the-shelf components and instruments. The measurement technique described consists of a double-balanced mixer used as phase detector, followed by a low noise amplifier. An FFT spectrum analyzer is then used to view the modulation components. A simple calibration procedure is outlined that ensures accurate measurements. A block diagram of the configuration is presented as well as actual phase noise data from the 400-kW, 2.115-GHz (S-band) klystron transmitter.

I. Introduction

Various papers (Refs. 1 and 2) contain outlines of methods to measure transmitter phase stability. This article describes the implementation of the phase detector method, with particular emphasis on close-in phase noise measurement. Practical problems encountered during such a measurement are also described. Simple, accurate, and easily reproducible measurements are necessary so that improved transmitter designs can evolve.

Unwanted modulation and noise in the transmitted RF signal are caused by a variety of sources – specifically, shot noise in the klystron, fluctuations in the cathode beam power, RF drive power, and heater supply voltages, cooling water temperature fluctuations, focus supply fluctuations, and mechanically induced vibrations from cooling fans and water pumps. These pertubations will in most cases produce both angle and amplitude modulation. However, in klystron amplifiers, near the carrier, angle modulation (phase noise) predominates.

The most significant source of phase error is generally the cathode voltage applied to the klystron. As the cathode voltage increases and decreases, the corresponding increase and decrease in electron beam velocity create a decrease and increase in the apparent electrical length of the tube. This results in a higher quantity of electrons being emitted, which in turn produces an increase in amplitude of the RF output. Generally, as stated earlier, any amplitude disturbance is an order of magnitude less significant than the phase change and can therefore be ignored.

Another factor that introduces apparent change in phase length of the linear beam tube is the focusing magnet. As the electron beam enters the magnetic field, any component of the magnetic field which is perpendicular to electron velocity creates a transverse velocity component of the electrons. Since the energy of the electrons is conserved, any transverse velocity component that is added will detract from the axial velocity component, thus causing an apparent increase in the electrical length of the tube.

The RF drive amplitude variation is another factor which induces phase delay in the klystron amplifier; it is dependent on the tube gain (number of cavities), how close the tube is run to saturation, and the operating frequency of the tube. Since variation in drive power results in extracting more or less energy from the electron beam, there are corresponding changes in the beam velocity that induce phase changes.

Variations in heater voltages, which will change cathode temperature, will also have an effect on the phase error. Similarly, variations in the klystron body temperature will affect the length of the circuit and thus will also affect the phase error.

Finally, one must consider such effects as vibration in the tube from mechanical cavity tuner mechanisms that can physically move due to vibration or antenna movement. In addition, physical vibration of coaxial cables, couplers, and similar components should be considered.

II. Noise Spectrum

A frequency domain representation of a CW carrier with noise sidebands is shown in Fig. 1. The vertical scale represents the ratio of single sideband (SSB) power in a 1-Hz bandwidth, at a frequency *fm* away from the carrier, to the total signal power. This quantity is given the symbol $\mathcal{L}(f)$, with units dBc/Hz (dB below carrier in a 1-Hz bandwidth). Noise power varies directly with measured bandwidth. Thus, noise measured in a bandwidth other than 1 Hz may be normalized to a 1-Hz bandwidth by subtracting the correction factor given in Eq. (1).

$$\text{Correction Factor} = 10\log_{10}\frac{\text{BW}}{1\ \text{Hz}} \tag{1}$$

where BW is the measured bandwidth in Hz. The power of discrete deterministic sidebands does not scale with measurement bandwidth; it remains constant.

As stated earlier, the phase noise in a klystron dominates *am* noise at frequencies close to the carrier, and to measure this noise the phase detector method was used.

III. Phase Detector Method

The theory behind this measurement is fairly straightforward. The basic components are a double balanced mixer used as a phase detector, a low noise amplifier, and a low frequency spectrum analyzer. The relationship between the RMS variation in phase between the LO and RF ports of the mixer and the ratio of the power in a single sideband to the power in the carrier (P_{SSB}) is given by:

$$P_{SSB} = \frac{\phi^2}{2}$$

where ϕ is the difference between the RF and LO ports. Also, the relationship between the IF voltage (V_{IF}) of the mixer and ϕ is given by:

$$\begin{aligned} V_{IF} &= K\cos(\pi/2 + \phi\ \text{rms}) \\ V_{IF} &\cong K\,\phi\ \text{rms} \end{aligned} \tag{2}$$

where K is the mixer sensitivity and

$$V_m = AV_{IF}$$

where A is the LNA gain and

$$P_{SSB} = \frac{V_m^2}{2(AK)^2}$$

This is valid only for phase deviations of less than 0.1 radians.

Thus, by measurement of V_m and knowledge of the characteristics of the circuit (A and K), the noise spectrum can be determined.

IV. Hardware

A complete block diagram of the measurement system is shown in Fig. 2. Several elements must be added to the simple circuit described earlier to allow an accurate measurement. Circulators to provide a matched impedence, attenuators to control the power level, and couplers to monitor the power level should be placed at both the LO and RF ports of the mixer. A phase shifter to control the offset phase should be placed in the RF side of the mixer circuit. A bias tee should be placed at the IF port of the mixer to provide a non-reactive termination. It was also found necessary to place a 1 kohm resistor from the output of the bias tee to ground to increase the low frequency sensitivity of the mixer. In addition, a DC blocking capacitor was needed to prevent any DC offset from the mixer from forcing the high gain LNA to saturate. One should also consider the noise contribution of the test system elements. When selecting elements such as the driving source (i.e., the LO signal) and the low noise amplifier, care should be taken to choose generators and amplifiers that will not contribute significant noise compared to what is being measured. An HP 3561 A dynamic signal analyzer was used as the low frequency spectrum analyzer.

V. Calibration

A simple method of calibration was chosen so that it was not necessary to determine all the parameters of the measurement system. The system was calibrated by injecting a known phase-modulated signal and measuring the results. This is performed for all modulation frequencies of interest in order to form a calibration curve for the circuit at the frequencies of interest. For accurate results, it is important that the signal modulation be fairly pure phase modulation of a known P_{SSB} level. In calibrating the circuit, a P_{SSB} ratio of -30 dB was used with higher order sidebands at -50 dBc or lower. This level is set with an RF spectrum analyzer and modulating at a frequency that can be seen. The modulation frequency was then stepped from 100 kHz down to 0.01 Hz and the sideband observed with the low frequency FFT analyzer. For system calibration, the analyzer was used in the narrow-band mode to read the actual values of the modulation sidebands.

It was found that the major contributor to any frequency roll-off is the high-pass filter formed by the DC blocking capacitor and the combination of the corresponding circuit element resistances. This can be fairly well modeled by a simple RC filter whose corner frequency is about 2 Hz. The response also falls off a little at frequencies higher than 60 Hz, but since the main frequencies of interest for this measurement are below 20 kHz, this effect can be neglected. This response will then be used to correct the measured data.

VI. Measurement

When setting up the system to make a measurement, care must be taken to match the calibration conditions as closely as possible. The power levels seen by the mixer at its RF and LO ports are especially critical. Values of P_{LO} = +8 dBm and P_{RF} = -2 dBm were chosen for this measurement. These values can be changed but they must be repeated between calibration and an actual measurement.

The mixer must also be in quadrature for maximum sensitivity to phase variations and minimum sensitivity to amplitude variations. This is determined by monitoring the mixer IF voltage before the DC blocking capacitor. Because it can take hours to make a measurement at low frequency spans, it is desirable to know about any long-term phase drifts. An attempt was made to continuously monitor this point to check for very long-term phase drifts, but this led to problems because the spectrum analyzer was able to detect noise from the instrument used to monitor this point. Quadrature was then checked before and after the measurement in order to detect unacceptable amounts of drift.

The measurement was made at seven different frequency spans. The data for each of these spans was then combined to form one plot. These frequency ranges were:

0–100 kHz

0–10 kHz

0–1 kHz

0–100 Hz

0–10 Hz

0–1 Hz

0–0.1 Hz

The measurement data for each frequency span was read from the spectrum analyzer into the computer, where any gain or attenuation effects imposed by the system and determined in the calibration were weighted out. This provided results in the form of dBc/Hz. Each frequency span consists of 400 data points, which provides single-point resolution of 0.25 mHz on the 0.1 Hz frequency span.

When making this measurement, the spectrum analyzer will automatically range to accommodate the largest noise signal seen at its input. If there are relatively high-level discrete lines, the analyzer will choose a range to accommodate these signals. Since the dynamic range of the analyzer is 80 dB, low-level random noise cannot be detected when these discrete lines are present. Although the noise per Hz typically rises as one approaches the carrier, this effect is overwhelmed by the low frequency roll-off of the measurement system, and by the decreasing measurement bandwidth.

To avoid the above problem, which was caused by cathode voltage power supply lines and other discrete lines, a low-pass filter was used for spans less than 10 Hz. The filter had a corner frequency of about 2 Hz, and its effect was corrected for in the data measured at 1 Hz or less.

Since the spectrum analyzer was capable of storing the time data as well as the frequency data, the measurement was done using this "time buffer" capability. The time data can then be searched for any one-time event such as a step in phase. Events of this type can cause very deceptive results in the measured noise level. This method, although helpful, requires the storing and handling of large amounts of data.

VII. Measured Data

Figure 3 shows the results of the phase noise measurement made on the class C driver amplifier. It should be noted that this follows a theoretical $1/f$ noise characteristic. It is also

apparent that the driver noise is approximately 20 dB lower than the noise measured with the klystron in the circuit. This plot is shown in Fig. 4. The plot of the transmitter phase noise reveals several discrete spurious lines. Most of these components are traceable to the cathode voltage noise characteristics, which are shown in Fig. 5. The dominant lines are at 400 Hz due to the generator frequency, at 800 Hz (the 2nd harmonic), and at 2400 Hz (a product of the 400-Hz rectification). Also present is an unexpected line at 16 Hz, which was found to be a product of the cathode voltage supply's control feedback loop.

When the cathode supply voltage noise spectrum and the phase noise spectrum are compared, it becomes apparent that the two are very similar. This implies that the supply voltage is the major contributor to the noise. This is expected because the cathode voltage has the highest phase pushing factor of the affecting parameters. It is also seen that the noise of the system approaches the noise of the driver amplifier at high frequencies.

VIII. Conclusions

This article has presented a technique for measuring the phase noise of RF power amplifiers that is easily reproducible using off-the-shelf instruments and common electronic components. Measurement results are readily interpreted and unambiguous. This method will assist in the design evolution process (improved power supply regulation and long-term stability, improved temperature control of the cooling water, etc.) by correlating design changes with overall performance measurements.

Acknowledgments

The authors acknowledge the assistance of Marlyn Gregg and John Daeges in performing the measurements and interpreting the data.

References

1. Nocella, P. (Sperry Corporation), "Practical Purity Measurement of Pulse Doppler Radar Transmitter Amplifiers," *IEEE 17th Pulse Power Modulator Symposium, 1986*, pp. 32–38.
2. "Spectrum Analysis Noise Measurements," *Hewlett-Packard Application Note 150-4*, Palo Alto, California, April 1974.

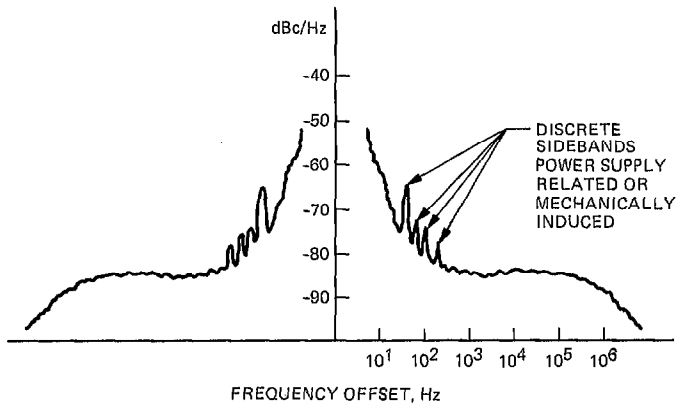

Fig. 1. The CW phase noise

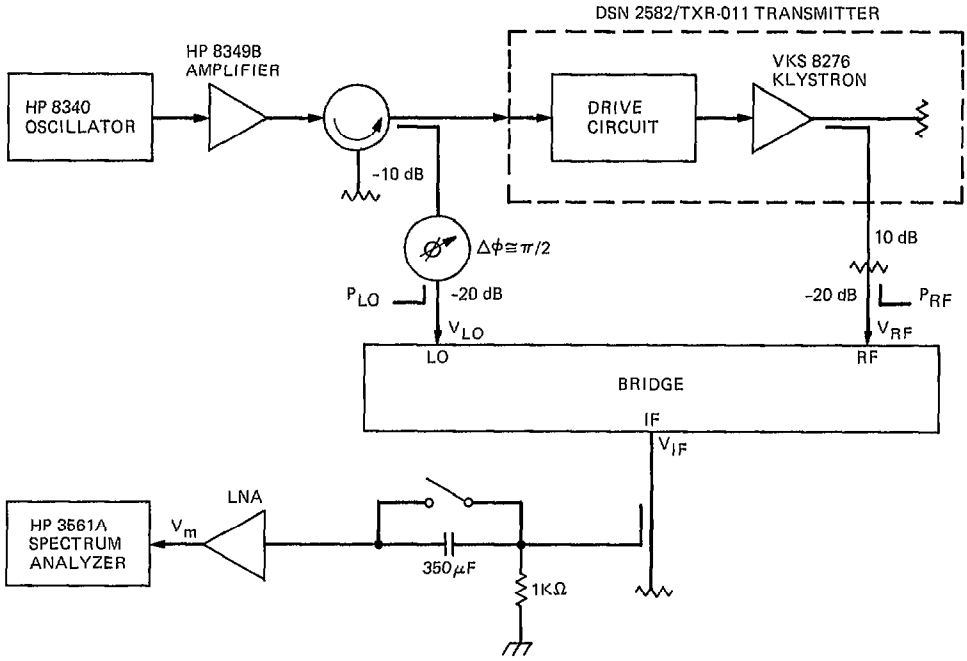

Fig. 2. Phase noise measurement system

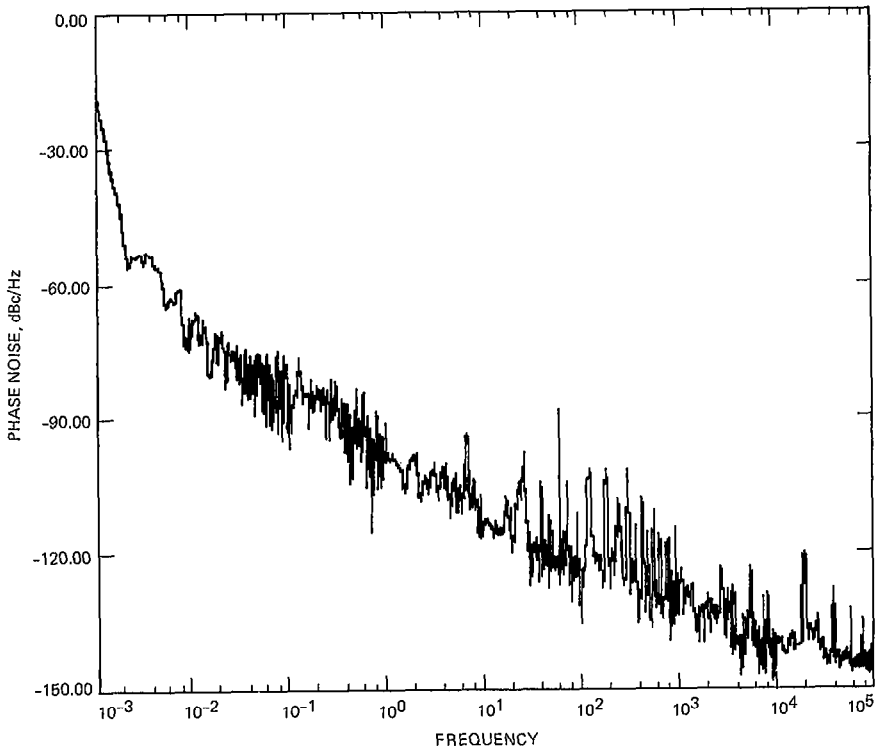

Fig. 3. Class C driver amplifier phase noise

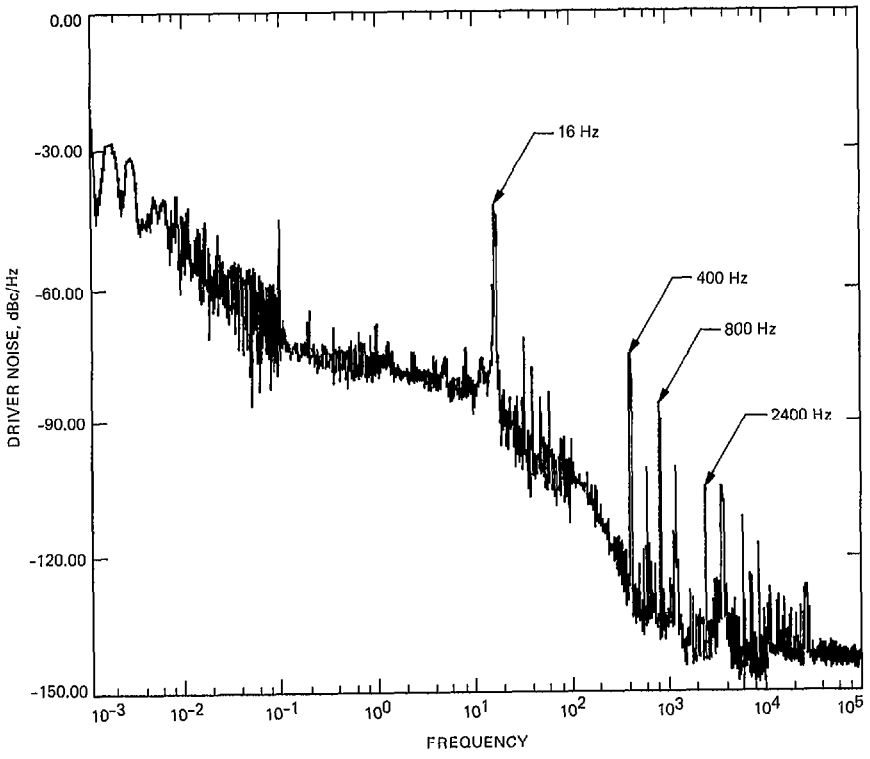

Fig. 4. The 2.115-GHz, 400-kW transmitter phase noise

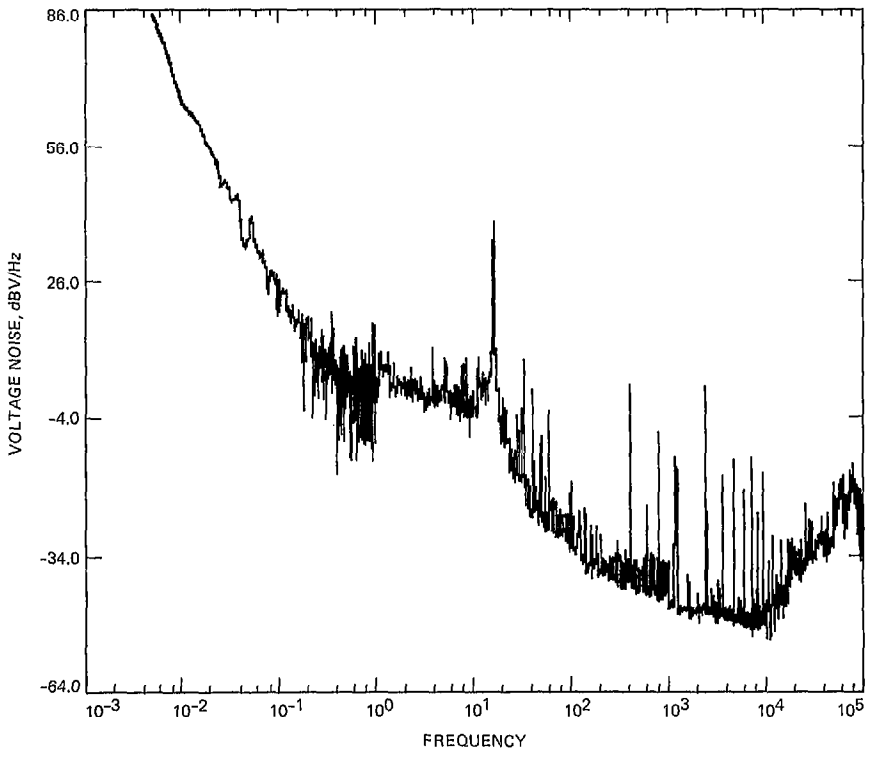

Fig. 5. Cathode voltage supply noise spectrum